Effects of Weather Variability and Soil Parameter Uncertainty on the Soil–Crop–Climate System

ANGELOS L. PROTOPAPAS

Polytechnic University, Brooklyn, New York

RAFAEL L. BRAS

Massachusetts Institute of Technology, Cambridge, Massachusetts

(Manuscript received 17 June 1991, in final form 14 June 1992)

ABSTRACT

The variability of crop and soil states due to uncertain climatic inputs and soil properties is quantified using a mathematical representation of the physiological, biochemical, hydrological, and physical processes related to plant growth. The components of the state-space model of the soil–crop–climate interactions are a plant growth, a moisture transport, and a solute transport model. A linear model for the perturbations of the state and the inputs around the nominal (first-order mean) values is derived. The linear model is used for second-moment uncertainty propagation due to fluctuations of the climatic forcing in time and due to the spatial variability of the soil properties. The most important climatic variables affecting crop production are identified in a case study. Correlation of climatic inputs between days is found to increase the crop yield variance. Significant variance reduction is found in transforming random soil properties to soil-state variables and then to plant-state variables.

1. Introduction

The complex interactions that take place in a cropped land surface transforming solar energy into organic matter are affected by uncertainties of varied degree and origin. The objective of this study is to quantify the variability of crop and soil variables due to uncertain climatic inputs and soil parameters, not from an empirical, statistical point of view, but based on a mathematical representation of the physiological, biochemical, hydrological, and physical processes that result in plant growth. Such information is useful for assessing the impact of climatic change on vegetation and also for improving agricultural practices, for example, irrigation scheduling and crop planning.

Theoretical modeling of the climate, soil, and vegetation interactions in a stochastic, analytical framework has been advanced by Eagleson (1978a–g). In his study, the mean and the variance of the annual hydrologic fluxes are computed as functions of soil and climatic variables. Several physically based models for dynamic simulation of the seasonal growth of crops as related to moisture and salinity conditions in the soil have been proposed (Childs et al. 1977; Zur and Jones 1981; Huck and Hillel 1983; Ritchie and Otter 1985; Bresler and Dagan 1988). All these models are presented in the form of simulation computer programs, and are therefore not suitable for analytical work.

Studies that review temporal variability of crop yield take the form of statistical analyses of records of annual yield for a specific crop and site. Spatial variability studies of crop yield are historically related to early results on random fields. Whittle (1956), analyzing crop yield data as a realization of a stationary stochastic process, discovered that the correlation function falls off relatively slowly at large distances. Recently, attention has been paid to the relation between soil property and crop variability at field scale. The statistical analysis of Bresler et al. (1981) finds the auto- and cross correlations of soil properties and crop yield components. Similar statistical analysis on field data is reported by Russo (1984b), including salinity measurements.

Warrick and Gardner (1983) use a relation between yield and water to predict mean yield, based on a derived distribution approach. They do not consider soil salinity, irrigation water salinity, spatial variation of the soil properties, or any dependence on climate. Russo (1983) favors a geostatistical modeling approach. The semivariograms of the saturated hydraulic conductivity and of the capillarity index are found from point measurements on a crop field. Kriging is employed to estimate the values of these parameters over the entire field. Then, the soil water potential h_c is mapped and is found to be highly correlated to the

Corresponding author address: Dr. Angelos L. Protopapas, Department of Civil and Environmental Engineering, Polytechnic University, 6 Metrotech Center, Brooklyn, NY 11201.

capillarity index. A quadratic dependence of crop yield on h_c is assumed. Yield is found to be less variable than h_c and with an integral scale close to the arithmetic mean of the integral scales of the soil properties. Field experiments (Russo 1984a) verify the predictions of this model.

Following up on this approach Russo (1986) attempts a more detailed representation of soil–crop–climate interactions by using simplified water and solute dynamics and a yield-transpiration model. Using generated realizations of the soil properties and the crop response model, conditional simulations are performed. Bresler and Dagan (1988a,b) and Dagan and Bresler (1988) present a methodology to predict the variability of crop yield due to uncertain soil and crop parameters. They use a yield-transpiration model combined with soil-column models for flow and transport distributed vertically. Second-moment analysis is used to obtain the yield variance.

The work of Protopapas and Bras (1986), Protopapas (1988), and Protopapas and Bras (1988) suggests an integrated model of the soil–crop–climate interactions, which is based on the underlying physical processes. Soil moisture and salinity profiles are predicted solving the distributed parameter governing equations for flow and transport in the unsaturated zone. Crop yield is predicted by explicitly modeling the plant growth processes, such as assimilation, respiration, and transpiration. The model is developed in an analytical state–space form, that is, as a set of nonlinear equations for the propagation of the plant- and soil-state variables. As will be seen in the following sections, this formulation is convenient for implementation of uncertainty propagation methods.

This paper includes six additional sections. Section 2 presents the system model and summarizes the linearization method. Sections 3 and 4 deal with the effects of weather variability and sections 5 and 6 discuss the effects of soil parameter variability. Section 7 summarizes our conclusions and future research directions.

2. Linearization of the soil–crop–climate model

The conceptual basis for modeling the growth of a crop is summarized as follows. The climatic inputs act on the canopy of the crop, resulting in photosynthesis and transpiration. The products of photosynthesis are the reserves of the plant and are utilized for maintenance and growth of the shoot and root biomass. The transpiration demand is met by water uptake through the root system at a rate that largely depends on the moisture and salinity conditions in the soil. By adjusting its water content (or equivalently its water potential) the plant balances demand and uptake, and at the same time regulates the partitioning of biomass in shoot and root. The water and salt transport in the soil establishes the conditions for water uptake by the root system. In Protopapas and Bras (1988) these concepts have been quantified and expressed mathematically, following ideas and data reported in de Wit et al. (1978). The vertical distribution of the root system, the soil moisture, and the salinity over depth is explicitly considered. As state of the system at time κ we define a vector

$$x_\kappa = [\psi_p \mathrm{RES} W_S \vdots RT_{y1} \cdots RT_{yN} \vdots RT_{o1} \cdots RT_{oN} \vdots \psi_1 \cdots \psi_N \vdots c_1 \cdots c_N]^{\mathrm{T}},$$

with dimensions $3 + 4N$ by 1, where N is the number of the discretization nodes over depth; ψ_p is the plant water potential (in bars), characterizing the water status of the plant; RES is the weight of reserves (in kg ha^{-1}); W_S is the weight of shoot (in kg ha^{-1}); RT_{yj} and RT_{oj} are the young and old root weight at node j (in kg ha^{-1}); ψ_j is the soil matric potential (in cm) characterizing the water content of the soil; and c_j is the soil salinity (in mg l^{-1}).

We further introduce a vector of climatic inputs

$$\xi_\kappa = [R_n R_v T_a T_d T_s u R_s]^{\mathrm{T}},$$

where ξ_κ is the seven-dimensional input vector at time κ; R_n, R_v, and R_s are the net absorbed solar radiation, the photosynthetically active radiation, and the net radiation at the soil surface, respectively (in J m^{-2} s^{-1}); T_a, T_d, and T_s are the air temperature, the dewpoint temperature, and the soil temperature, respectively (in °C); and u is the wind speed (in m s^{-1}).

Finally, we define an nN-dimensional vector of soil parameters ζ to describe the hydraulic properties of the soil at each node j, where n is the number of required soil parameters.

The state is partitioned into plant- and soil-state variables

$$x(\kappa) = [x_p(\kappa) \vdots \psi(\kappa) \vdots c(\kappa)]^{\mathrm{T}},$$

where $x_p(\kappa)$ has the first $3 + 2N$ plant-related variables, and $\psi(\kappa)$ and $c(\kappa)$ collectively denote the matric potential and concentration values at all nodes.

The propagation equations for each plant-state variable are derived in Protopapas and Bras (1988), giving a nonlinear, time-varying state–space model:

$$x_p(\kappa + 1) = f_p[x_p(\kappa), \xi(\kappa), \psi(\kappa), c(\kappa)]. \quad (1)$$

The discretization of the flow equation leads to a system

$$\mathbf{A}_f[\psi(\kappa), \zeta]\psi(\kappa + 1) = \mathbf{e}[\psi(\kappa), \zeta, x_p(\kappa), \xi(\kappa)], \quad (2)$$

and the discretization of the solute transport equation leads to a system

$$\mathbf{A}_t[\psi(\kappa), \zeta]c(\kappa + 1) = \mathbf{B}_t[\psi(\kappa), \zeta]c(\kappa), \quad (3)$$

where the matrices $\mathbf{A}_f$, $\mathbf{A}_t$, and $\mathbf{B}_t$ and the vector $\mathbf{e}$ have proper dimensions. Matrices $\mathbf{A}_f$ and $\mathbf{A}_t$ are tridiagonal and can be inverted analytically and explicitly (Protopapas 1988) in order to isolate $\psi(\kappa)$ and $c(\kappa)$ in the

left-hand side of Eqs. (2) and (3). Then the model can take the form

$$x(\kappa + 1) = \mathbf{f}_\kappa[x(\kappa), \xi(\kappa), \zeta]. \quad (4)$$

Variability of the climatic inputs in time and of the soil parameters in space may corrupt the predictions of the state–space nonlinear time-varying model given by the system of Eq. (4). It is unrealistic to obtain a complete statistical characterization of the output of such dynamic systems. There are, however, available techniques for predicting second-moment properties of the outputs given second-moment information about the inputs. Broad families of such techniques are Monte Carlo methods, derived distribution methods, and linearization methods.

In this study a linearization method is used to propagate uncertainty in the soil–crop–climate model. Although the method is approximate, typically it is more efficient computationally than Monte Carlo methods due to its analytical nature. Given a state–space model of the system [Eq. (4)], a linearized model for the fluctuations of the inputs and outputs around nominal values is derived by expanding in Taylor's series up to first order. Then moment propagation methods can be used with the linearized system.

The plant system [Eq. (1)] can be linearized along a nominal trajectory (denoted by $\hat{}$), which is taken to be the simulated values of the state and the nominal inputs, leading to a model for the fluctuations $x'_p = x_p - \hat{x}_p$, $\psi' = \psi - \hat{\psi}$, $\xi' = \xi - \hat{\xi}$, etc. and

$$x'_p(\kappa + 1) = \mathbf{A}_{1p}(\kappa)x'_p(\kappa) + \Lambda_p(\kappa)\xi'(\kappa) + \mathbf{A}_{2p}(\kappa)\psi'(\kappa) + \mathbf{A}_{3p}(\kappa)c'(\kappa). \quad (5)$$

Matrices $\mathbf{A}_{1p}(\kappa)$, $\Lambda_p(\kappa)$, $\mathbf{A}_{2p}(\kappa)$, and $\mathbf{A}_{3p}(\kappa)$ require the evaluation of the first-order derivatives of the propagation functions with respect to the state components and the climatic inputs at time κ.

Similarly, we obtain for the flow model [Eq. (2)]

$$\mathbf{A}_f[\hat{\psi}(\kappa), \hat{\zeta}]\psi'(\kappa + 1) = \mathbf{B}_f[\hat{\psi}(\kappa + 1), \hat{\psi}(\kappa), \hat{\zeta}, \xi(\kappa)] \times \psi'(\kappa) + \mathbf{H}_f[\hat{\psi}(\kappa + 1), \hat{\psi}(\kappa), \hat{\zeta}]\zeta' + \Pi_f[\hat{\xi}(\kappa)]\xi'(\kappa) + \Gamma_f[\hat{\psi}(\kappa), \hat{x}_p(\kappa)]c'(\kappa) + \mathbf{Z}_f[\hat{\psi}(\kappa), \hat{x}_p(\kappa)]x'_p(\kappa), \quad (6)$$

and for the transport model [Eq. (3)]

$$\mathbf{A}_t[\hat{\psi}(\kappa), \hat{\zeta}]c'(\kappa + 1) = \mathbf{B}_t[\hat{\psi}(\kappa), \hat{\zeta}]c'(\kappa) + \mathbf{C}_t[\hat{\psi}(\kappa), \hat{\zeta}, \hat{c}(\kappa + 1), \hat{c}(\kappa)]\psi'(\kappa) + \mathbf{H}_t[\hat{\psi}(\kappa), \hat{\zeta}, \hat{c}(\kappa + 1), \hat{c}(\kappa)]\zeta', \quad (7)$$

where $\mathbf{B}_f$, $\mathbf{H}_f$, Π_f, Γ_f, $\mathbf{Z}_f$, $\mathbf{B}_t$, $\mathbf{C}_t$, and $\mathbf{H}_t$ are matrices with proper dimensions. Matrices $\mathbf{A}_f$ and $\mathbf{A}_t$ remain unchanged and can be explicitly inverted.

From Eqs. (5), (6), and (7), the following linear perturbation system is obtained

$$\begin{bmatrix} x'_p(\kappa + 1) \\ \psi'(\kappa + 1) \\ c'(\kappa + 1) \end{bmatrix} = \begin{bmatrix} \mathbf{A}_{1p} & \mathbf{A}_{2p} & \mathbf{A}_{3p} \\ \mathbf{A}_f^{-1}Z_f & \mathbf{A}_f^{-1}\mathbf{B}_f & \mathbf{A}_f^{-1}\Gamma_f \\ 0 & \mathbf{A}_t^{-1}\mathbf{C}_t & \mathbf{A}_t^{-1}\mathbf{B}_t \end{bmatrix} \begin{bmatrix} x'_p(\kappa) \\ \psi'(\kappa) \\ c'(\kappa) \end{bmatrix} + \begin{bmatrix} \Lambda_p \\ \mathbf{A}_f^{-1}\Pi_f \\ 0 \end{bmatrix} \xi'(\kappa) + \begin{bmatrix} 0 \\ \mathbf{A}_f^{-1}\mathbf{H}_f \\ \mathbf{A}_t^{-1}\mathbf{H}_t \end{bmatrix} \zeta', \quad (8)$$

or

$$x'(\kappa + 1) = \mathbf{A}(\kappa)x'(\kappa) + \Lambda(\kappa)\xi'(\kappa) + \Gamma(\kappa)\zeta', \quad (9)$$

where x', ξ', and ζ' are vectors with dimensions $3 + 4N$ by 1, 7 by 1, and nN by 1, respectively, and $\mathbf{A}$, Λ, and Γ are matrices with dimensions $3 + 4N$ by $3 + 4N$, $3 + 4N$ by 8, and $3 + 4N$ by nN, respectively, with N the number of discretization nodes and n the number of the required soil parameters.

The first term in Eq. (9) describes the unforced dynamics of the system, the second term the effect of the variation of the climatic inputs, and the third term the effect of the soil properties. The linearization requires the definition of nominal values $\hat{x}(\kappa)$, $\hat{\zeta}$, and $\hat{\xi}(\kappa)$, at which the first-order derivatives are evaluated to define matrices $\mathbf{A}(\kappa)$, $\Lambda(\kappa)$, and $\Gamma(\kappa)$. The details on the linearization step are given in Protopapas (1988). Assuming known initial state, the nominal trajectory $\hat{x}(\kappa)$ can be simulated with the nonlinear model, given the inputs $\hat{\zeta}$ and $\hat{\xi}(\kappa)$.

Equation (9) is used to address the problem of how the variability of the climatic variables in time and of the soil properties in space affect the state of the system. The solution of Eq. (9) is

$$x'(\kappa) = \Phi(\kappa, 0)x'(0) + \sum_{\tau=0}^{\kappa-1} \Phi(\kappa, \tau + 1)\Lambda(\tau)\xi'(\tau) + \sum_{\tau=0}^{\kappa-1} \Phi(\kappa, \tau + 1)\Gamma(\tau)\zeta', \quad (10)$$

where the transition matrix $\Phi(\kappa, s)$ is defined from

$$\Phi(\kappa, s) = \mathbf{A}(\kappa - 1)\mathbf{A}(\kappa - 2)\cdots\mathbf{A}(s)$$

and $\Phi(\kappa, \kappa) = \mathbf{I}$, ($\mathbf{I}$ is the identity matrix).

3. Uncertainty of climatic inputs in time

Assuming that the soil parameters are known, Eq. (9) becomes

$$x'(\kappa + 1) = \mathbf{A}(\kappa)x'(\kappa) + \Lambda(\kappa)\xi'(\kappa), \quad x'(0) = 0 \quad (11)$$

with solution

$$x'(\kappa) = \sum_{\tau=0}^{\kappa-1} \Phi(\kappa, \tau + 1)\Lambda(\tau)\xi'(\tau). \quad (12)$$

Thus, the state perturbations are given by a linear time-varying system with the time series of the perturbations

of the climatic variables as forcing term. Using the following general second-moment characterization of the inputs

$$\bar{\xi}'(\kappa) = 0.0, \quad E[\xi'(\kappa)x'^{\mathrm{T}}(0)] = 0$$
$$\text{and} \quad E[\xi'(\kappa)\xi'(\eta)^{\mathrm{T}}] = \mathbf{H}(\kappa, \eta),$$

it follows that the mean $\bar{x}'$ and the covariance $\mathbf{P}_{x'x'}$ of the state perturbations can be found from

$$\bar{x}'(\kappa + 1) = \mathbf{A}(\kappa)\bar{x}'(\kappa),$$
$$P_{x'x'}(\kappa + 1) = \mathbf{A}(\kappa)\mathbf{P}_{x'x'}(\kappa)\mathbf{A}^{\mathrm{T}}(\kappa) + \Lambda(\kappa)\mathbf{H}(\kappa, \kappa) \times \Lambda^{\mathrm{T}}(\kappa) + \mathbf{A}(\kappa)E[x'(\kappa)\xi'^{\mathrm{T}}(\kappa)]\Lambda^{\mathrm{T}}(\kappa) + \Lambda(\kappa)E[\xi'(\kappa)x'^{\mathrm{T}}(\kappa)]\mathbf{A}^{\mathrm{T}}(\kappa). \quad (13)$$

Using Eq. (12) and taking expected values, the correlation between the state and the climate input is found as

$$E[x'(\kappa)\xi'^{\mathrm{T}}(\kappa)] = \sum_{\tau=0}^{\kappa-1} \Phi(\kappa, \tau + 1)\Lambda(\tau)E[\xi'(\tau)\xi'^{\mathrm{T}}(\kappa)] = \sum_{\tau=0}^{\kappa-1} \Phi(\kappa, \tau + 1)\Lambda(\tau)\mathbf{H}(\tau, \kappa). \quad (14)$$

To evaluate the summation in Eq. (14) and then the cross terms in Eq. (13), an assumption about the correlation structure of the disturbances is required.

In Protopapas (1988) the transformation from random daily climatic inputs to input sequences at a smaller time step (required for the simulation model) is discussed. Using both analytical considerations based on weather generators and Monte Carlo simulations it is found that within a daily cycle the output values of climatic variables are correlated at the the smaller time-step level. It is observed, however, that the fluctuations of the climatic variables from their mean values are isomorphic—during the day the fluctuations maintain a deterministic pattern, scaled by a random daily amplitude. Such sequences are shown to possess a separable covariance structure with possible correlation between different cycles (days) of length D. Three cases are considered in this study:

Case 1. Uncorrelated disturbances at each time step

The typical, yet not applicable to the problem at hand, choice of $\mathbf{H}(\tau, \kappa) = \mathbf{Q}(\kappa)\delta_{\tau\kappa}$ (where $\delta_{\tau\kappa}$ is the Kronecker delta which is 1 for $\tau = \kappa$ and 0 otherwise) vanishes the summation in Eq. (14) resulting in

$$\bar{x}'(\kappa + 1) = \mathbf{A}(\kappa)\bar{x}'(\kappa),$$
$$\mathbf{P}_{x'x'}(\kappa + 1) = \mathbf{A}(\kappa)\mathbf{P}_{x'x'}(\kappa)\mathbf{A}^{\mathrm{T}}(\kappa) + \Lambda(\kappa)\mathbf{Q}(\kappa)\Lambda^{\mathrm{T}}(\kappa), \quad (15)$$

with initial conditions $\bar{x}'(0) = 0$ and $\mathbf{P}_{x'x'}(0) = 0$.

Since $x(\kappa) = x'(\kappa) + \hat{x}(\kappa)$ it follows that

$$\bar{x}(\kappa) = \hat{x}(\kappa) \quad \text{and} \quad \mathbf{P}_{xx}(\kappa) = \mathbf{P}_{x'x'}(\kappa).$$

These results hold, however, under the restrictive assumption that the deviations $\xi'(\kappa)$ are uncorrelated at different time steps. In the case of climatic variables, it was found that this is not the case at time levels smaller than daily.

Case 2. Uncorrelated disturbances among different cycles

This is the case where the daily amplitude of a climatic variable is independent from its past values, and therefore the time step sequences among different cycles are uncorrelated or

$$\mathbf{H}(\tau, \kappa) = E[\xi'(\tau)\xi'(\kappa)^{\mathrm{T}}] = \begin{cases} \mathbf{Q}(\tau)\mathbf{Q}(\kappa)^{\mathrm{T}}, \\ \qquad \text{for} \quad \tau, \kappa \text{ in } [\mu D, (\mu + 1)D - 1] \\ 0, \quad \text{otherwise,} \end{cases} \quad (16)$$

where μ is the number of completed cycles (days) of length D from time 0 to time κ (which is equal to the integer part of κ/D).

In this case the summation in Eq. (14) starts at the beginning of each cycle, that is,

$$E[x'(\kappa)\xi'^{\mathrm{T}}(\kappa)] = \sum_{\tau=\mu D}^{\kappa-1} \mathbf{A}(\kappa, \tau + 1)\Lambda(\tau)\mathbf{Q}^{(\tau)}\mathbf{Q}^{\mathrm{T}}(\kappa) = \mathbf{N}(\kappa)\mathbf{Q}^{\mathrm{T}}(\kappa),$$

where

$$\mathbf{N}(\kappa) = \mathbf{A}(\kappa - 1)\mathbf{N}(\kappa - 1) + \Lambda(\kappa - 1)\mathbf{Q}(\kappa - 1);$$
$$\mathbf{N}(\mu D) = 0, \quad \kappa = \mu D + 1, \cdots, (\mu + 1)D. \quad (17)$$

Then Eq. (13) yields

$$\bar{x}'(\kappa + 1) = \mathbf{A}(\kappa)\bar{x}'(\kappa),$$
$$\mathbf{P}_{x'x'}(\kappa + 1) = \mathbf{A}(\kappa)\mathbf{P}_{x'x'}(\kappa)\mathbf{A}^{\mathrm{T}}(\kappa) + \Lambda(\kappa)\mathbf{Q}(\kappa)\Lambda^{\mathrm{T}}(\kappa) + \mathbf{A}(\kappa)\mathbf{N}(\kappa)\mathbf{Q}^{\mathrm{T}}(\kappa)\Lambda^{\mathrm{T}}(\kappa) + \Lambda(\kappa)\mathbf{Q}(\kappa)\mathbf{N}^{\mathrm{T}}(\kappa)\mathbf{A}^{\mathrm{T}}(\kappa). \quad (18)$$

Therefore by storing only the system and disturbance matrices, $\mathbf{A}(\kappa - 1)$ and $\Lambda(\kappa - 1)$, as well as the "square root" of the disturbance covariance matrix $\mathbf{Q}(\kappa - 1)$ at the previous time step, it is possible to compute $N(\kappa)$ from Eq. (17) and use it in Eq. (18) for all steps within a cycle. At the end of each cycle D, matrix $\mathbf{N}(\kappa)$ is set equal to zero and the computation continues.

Case 3. Correlated disturbances among different cycles

This is the case where the daily amplitude of a climatic variable is related to its past, and hence, there is memory in the daily process. The step sequences are correlated not only within a cycle, but also among different cycles, or

$$\mathbf{H}(\tau, \kappa) = E[\xi'(\tau)\xi'(\kappa)^{\mathrm{T}}] = \mathbf{Q}(\tau)\mathbf{M}_1\mathbf{Q}(\kappa)^{\mathrm{T}},$$
$$\text{for} \quad \begin{matrix} \tau \text{ in } [\mu D, (\mu+1)D - 1] \\ \kappa \text{ in } [(\mu+1)D, (\mu+2)D - 1], \end{matrix} \tag{19}$$

where $\mathbf{M}_1$ is the lag-one correlation matrix of the random amplitudes between cycles μ and $\mu + 1$. In this case it can be shown that the moment propagation equations are the same as Eq. (18), but matrix $\mathbf{N}(\kappa)$ is given from

$$\mathbf{N}(\kappa) = \mathbf{A}(\kappa - 1)\mathbf{N}(\kappa - 1) + \Lambda(\kappa - 1)\mathbf{Q}(\kappa - 1),$$
$$\mathbf{N}(0) = 0,$$
$$\mathbf{N}[(\mu+1)D] = \mathbf{N}[(\mu+1)D]\mathbf{M}_1. \tag{20}$$

That is, at the end of each cycle the matrix $\mathbf{N}(\kappa)$ is post multiplied by the one-lag correlation matrix between cycles and the calculation remains the same.

The implications of these three cases regarding the output variance and the developed recursive algorithm are illustrated with a scalar example in appendix A. Equations (15), (18), and (20) provide an algorithm for the propagation of the state covariance, which requires efficient implementation due to the high dimensionality of the involved matrices. In this study a sparse matrix multiplication algorithm reported by Gustavson (1978) is employed. The analysis and documentation of the algorithm can be found in Protopapas (1988).

4. Effects of weather variability

The proposed method for second-moment analysis of the crop- and soil-state variables as a result of temporal variability of the climatic inputs is applied in this section using parameters and field data for a maize crop planted in Flevoland (Netherlands, latitude 52°N) (de Wit et al. 1978). The available single realization of weather conditions at this site is assumed to represent the mean values of the climatic variables. Therefore, the results may be interpreted as a sensitivity study around this particular realization.

A single climatic variable is simulated in the model as

$$\xi(\kappa) = \alpha_d(\kappa)g(\kappa) + \beta_d(\kappa),$$

where $\beta_d(\kappa)$ is a deterministic constant during a day, $\alpha_d(\kappa)$ is a random daily amplitude, and $g(\kappa)$ is a deterministic shaping function. Using this model the variance is

$$\sigma^2_\xi(\kappa) = \sigma^2_{\alpha_d}(\kappa)g^2(\kappa) = \sigma^2_{\alpha_d}(\kappa)\left[\frac{\bar{\xi}(\kappa) - \beta_d(\kappa)}{\bar{\alpha}_d(\kappa)}\right]^2$$
$$= \left[\frac{\sigma^2_{\alpha_d}(\kappa)}{\bar{\alpha}_d(\kappa)}\right]^2 [\bar{\xi}(\kappa) - \beta_d(\kappa)]^2$$
$$= CV^2_{\alpha_d}[\bar{\xi}(\kappa) - \beta_d(\kappa)]^2. \tag{21}$$

Consequently, to compute the standard deviation of each climatic variable at time κ, the "reduced mean" $\bar{\xi}(\kappa) - \beta_d(\kappa)$ is multiplied by the coefficient of variation of the daily amplitude CV_{α_d}. The CV_{α_d} is taken constant at 0.66 for wind speed, 0.25 for the radiation fluxes, and 0.20 for air, dewpoint, and soil temperature.

In vector notation the transformation from the fluctuations of the daily random amplitude process to the smaller time-step process is

$$\xi'(\kappa) = \mathbf{G}(\kappa)\eta'(\kappa),$$

where $\mathbf{G}(\kappa)$ is a diagonal shaping matrix and $\eta'(\kappa)$ has zero mean and covariance matrix R. It can then be shown that the covariance of the climatic inputs ξ' has a separable form

$$\mathrm{cov}[\xi'(\kappa), \xi'(s)] = \mathbf{G}(\kappa)\mathbf{R}\mathbf{G}^{\mathrm{T}}(s)$$
$$= \mathbf{G}(\kappa)\Sigma\mathbf{L}\mathbf{L}^{\mathrm{T}}\Sigma^{\mathrm{T}}\mathbf{G}^{\mathrm{T}}(s)$$
$$= \mathbf{Q}(\kappa)\mathbf{Q}^{\mathrm{T}}(s),$$

where $\mathbf{Q}(\kappa) = \mathbf{G}(\kappa)\Sigma\mathbf{L} = \mathbf{G}(\kappa)\,\mathrm{diag}[\sigma_{\xi_i}(\kappa)]\mathbf{L}$, with $\mathbf{R} = \Sigma\mathbf{L}\mathbf{L}^{\mathrm{T}}\Sigma^{\mathrm{T}}$. Matrix Σ is a diagonal matrix with entries the standard deviations of each climatic input and $\mathbf{L}$ is a lower triangular matrix, which is the Cholesky decomposition matrix (square root) of the correlation coefficient matrix of the daily amplitudes (Bras and Rodriguez-Iturbe 1985). This structure allows the use of the procedure for covariance propagation developed in the previous section. At each time-step matrix, $\mathbf{Q}(\kappa)$ is computed by multiplying a diagonal matrix with entries the standard deviations of the climatic inputs [found from Eq. (21)] and matrix $\mathbf{L}$.

The standard deviation of the shoot weight and the reserve weight due to uncertain individual inputs is shown in Fig. 1, where no correlation among different days is used. The effect on the soil-state variables is minimal. In this application, salinity in the soil is zero and no irrigation is used. The input variables contributing most to output variance are absorbed visible radiation and air temperature, while soil temperature and dewpoint temperature have a moderate effect. Wind speed, net absorbed radiation, and radiation reaching the soil surface have minimal impact on the crop weights. In the same Fig. 1 the effect of all the inputs is shown, assuming that they are uncorrelated with each other. It is demonstrated that the effect of each climatic variable is not additive.

Introducing correlation of the amplitude of the absorbed visible radiation (which is found to affect yield variance most) among consequent days, the output variance increases as shown in Fig. 2. This suggests that crop production is more uncertain in areas where the realizations of the weather process during every growing season exhibit highly correlated fluctuations from day to day. If instead of such prolonged abnormalities the fluctuations are more random, the result is less-variable crop yields. In this particular simulation,

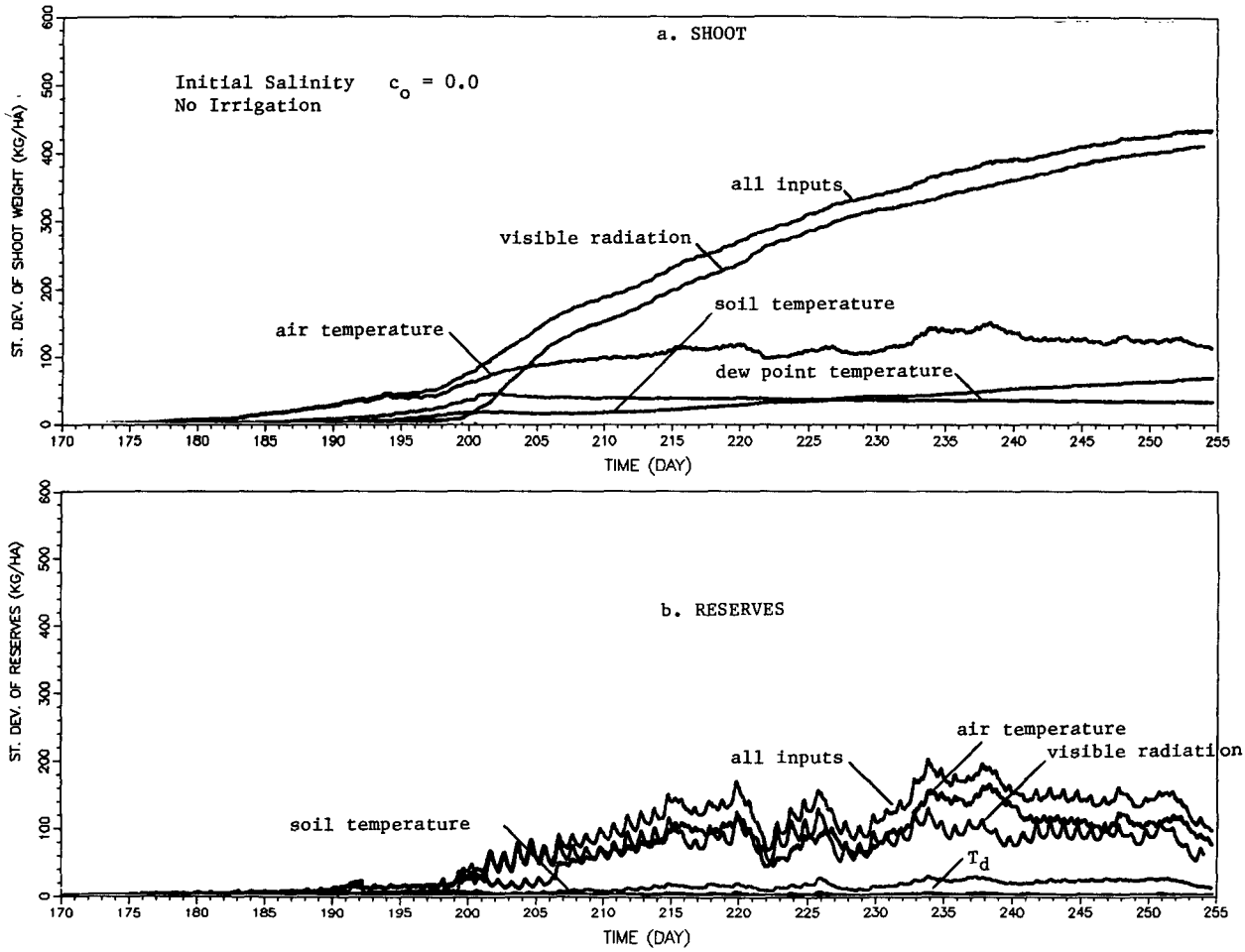

FIG. 1. Relative effect of uncertainty of particular inputs to the standard deviation of shoot (upper part) and reserves (lower part) ($c_0 = 0$, $r = 0$).

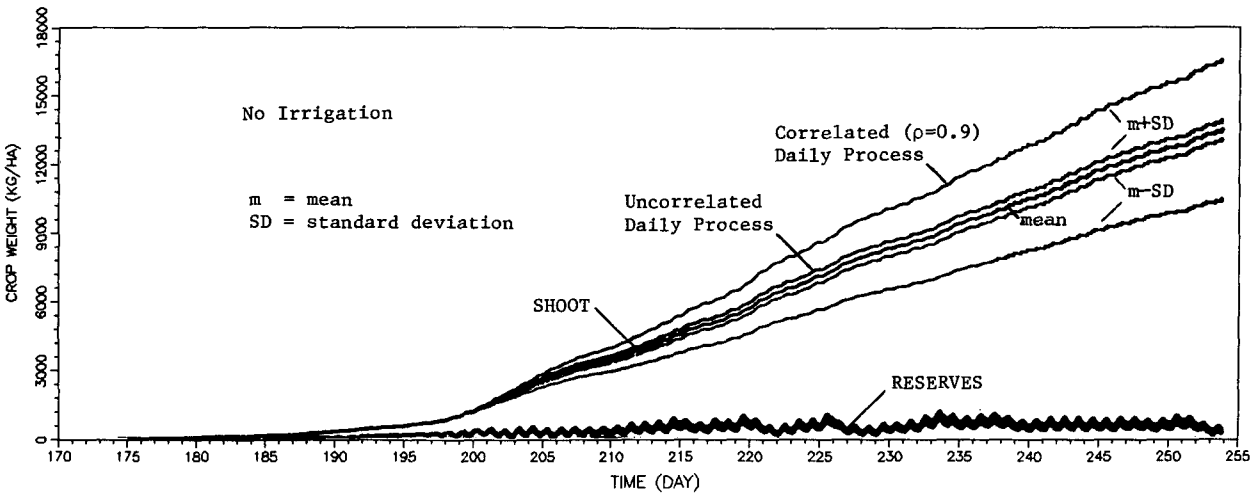

FIG. 2. Mean ± one standard deviation of state variables for the cases when the sequences of absorbed visible radiation are correlated or uncorrelated between days ($c_0 = 0$, $r = 0$).

introducing correlation increases the coefficient of variation of the shoot weight from 0.03 to 0.25.

5. Uncertainty of soil parameters in space

The solution of the unsaturated flow equation requires knowledge of the soil hydraulic properties, namely, the relation of unsaturated hydraulic conductivity $K(\psi)$ and of soil moisture $\theta(\psi)$ to the soil matric potential ψ. Different parameterizations of these relations have been proposed in the literature (see review by Russo 1988). A common model is

$$K(\psi) = K_s \exp(\alpha\psi),$$
$$\theta(\psi) = \theta_s \exp(\beta\psi), \quad (22)$$

where K_s is the saturated hydraulic conductivity (in cm day^{-1}) and α and β are empirical capillarity parameters (cm^{-1}).

Such expressions require only a small number of parameters, which usually exhibit spatial variability. In the last decade it has been recognized that these parameters can be represented by random fields with known statistical structure up to second moment. The linearization in section 2 was introduced in such a way that it can be used with any parameterization of the soil hydraulic properties, using the proper derivatives of the involved functions. The vector of soil parameters ζ, which is used in the soil–crop–climate model, contains the values of the parameters at each node over depth.

Assuming that the climatic inputs are known, Eq. (9) becomes

$$x'(\kappa + 1) = \mathbf{A}(\kappa)x'(\kappa) + \mathbf{\Gamma}(\kappa)\zeta', \quad \mathbf{x}'(0) = 0 \quad (23)$$

with solution

$$x'(\kappa) = \sum_{\tau=0}^{\kappa-1} \mathbf{\Phi}(\kappa, \tau + 1)\mathbf{\Gamma}(\tau)\zeta'. \quad (24)$$

Noticing that the $\zeta'(r)$ vector is time invariant and introducing a $3 + 4N$ by nN matrix $\mathbf{K}(\kappa)$, defined from

$$\mathbf{K}(\kappa) = \sum_{\tau=0}^{\kappa-1} \mathbf{\Phi}(\kappa, \tau + 1)\mathbf{\Gamma}(\tau), \quad (25)$$

Eq. (24) becomes

$$x'(\kappa) = \mathbf{K}(\kappa)\zeta', \quad (26)$$

which means that the state perturbations are a linear time-varying transformation of the random fields of the soil parameter perturbations. It is straightforward to show that

$$\mathbf{K}(\kappa) = \mathbf{A}(\kappa - 1)\mathbf{K}(\kappa - 1) + \mathbf{\Gamma}(\kappa - 1), \quad \text{with} \quad \mathbf{K}(0) = 0. \quad (27)$$

Matrix $\mathbf{K}(\kappa)$ is a deterministic quantity, which depends on the unforced system dynamics [matrices $\mathbf{A}(\kappa)$] and on the specific way that the soil properties affect the solution of the model [matrices $\mathbf{\Gamma}(\kappa)$]. Matrix $\mathbf{K}(\kappa)$, also named "total sensitivity," is independent of the statistical description of the soil variability. This matrix can be precomputed and stored at any time of interest and then used with any second-moment structure of the soil parameter fluctuations.

Assuming that the soil parameters are second-order stationary with mean $\bar{\zeta}$ and covariance function matrix $\mathbf{P}_{\zeta\zeta}(r, r + \chi) = \mathbf{P}_{\zeta\zeta}(\chi)$, we get

$$\bar{\zeta}' = 0, \quad \mathbf{P}_{\zeta'\zeta'}(\chi) = \mathbf{P}_{\zeta\zeta}(\chi),$$

and from Eq. (25)

$$\bar{x}'(\kappa) = 0,$$
$$\mathbf{P}_{x'x'}(\chi, \kappa) = \mathbf{K}(\kappa)\mathbf{P}_{\zeta\zeta}(\chi)\mathbf{K}^{\mathrm{T}}(\kappa). \quad (28)$$

Since $x(\kappa) = x'(\kappa) + \hat{x}(\kappa)$, it follows that

$$\bar{x}(\kappa) = \hat{x}(\kappa),$$
$$\mathbf{P}_{xx}(\chi, \kappa) = \mathbf{P}_{x'x'}(\chi, \kappa) = \mathbf{K}(\kappa)\mathbf{P}_{\zeta\zeta}(\chi)\mathbf{K}^{\mathrm{T}}(\kappa). \quad (29)$$

6. Effects of soil parameter uncertainty

The proposed method for second-moment analysis for spatially varying soil parameters is applied in this section for the maize crop in Flevoland (Netherlands). The root system is assumed to develop uniformly to a depth of 75 cm. The soil is assumed to be a Panoche clay loam with soil properties as reported in Warrick et al. (1971), which fit the exponential forms with parameters $K_s = 225$ cm day^{-1}, $\alpha = 0.04$ cm^{-1}, $\theta_s = 0.43$, and $\beta = 0.003$ cm^{-1}. For a local uniform soil-column model, K_s is assumed to be lognormally distributed with mean $\bar{K}_s = 225$ cm day^{-1} and variance $\sigma^2_{K_s}$. The uniformity assumption implies that K_s is perfectly correlated with depth.

The initial condition for soil moisture is a uniform value of 0.30 down to 50-cm depth, and then a linear increase to a value of 0.37 at 125 cm. The simulation starts on day 175 and ends on day 253. In a first example the initial salt concentration profile is uniform at a value of 3000 mg l^{-1} and no irrigation is applied. Using $\sigma^2_{K_s} = (300 \text{ cm day}^{-1})^2$, the prediction of the linearized model every 25 days is shown in Fig. 3, where one-standard-deviation bounds are plotted above and below the mean profiles of matric potential ψ (upper part) and solute concentration c (lower part). The use of the predicted variance to define such confidence intervals is only indicative for nonlinear systems.

The first ψ profile (day 175) corresponds to 12 h after the beginning of the simulation and shows a stationary behavior of the variance in space. At day 200, the soil dries up by free drainage at the bottom and evaporation at the surface (roots do not uptake much water during the first 25 days), and the variance of ψ increases and remains stationary. As roots start to

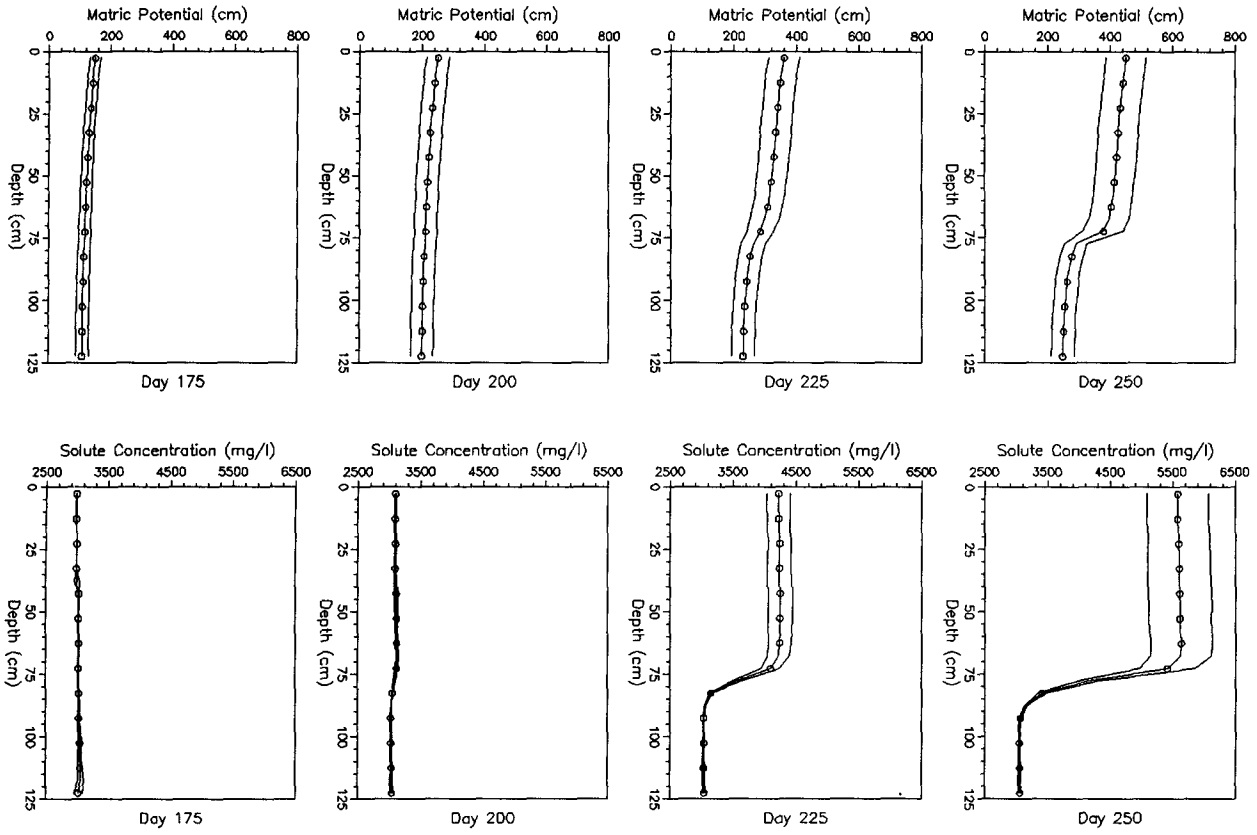

FIG. 3. Mean ± one-standard-deviation profiles of matric potential (upper part) and solute concentration (lower part), using the linearization method (K_s perfectly correlated over depth) (c_0 = 3000 mg l^{-1}, $r = 0$).

function and water is extracted preferentially from the upper 75 cm of soil (root zone), the soil becomes drier and the variance increases further.

The concentration profiles corresponding to days 175 and 200 show very small variance. During this period solute transport is mainly due to the dynamics of flow: the solutes are advected and dispersed. At day 225 the salts have built up due to decrease in moisture in the root zone and concentration variance increases with time in the root zone.

To check these results, a Monte Carlo method to predict uncertainty is used—one hundred values of saturated hydraulic conductivity K_s are sampled from its distribution and the nonlinear simulation is performed. Then the simulation results are averaged to calculate the statistics of the state variables. The computed means and variances of ψ and c compare well to the linearization results, although for day 225 and 250 the Monte Carlo method predicts less variance.

The variance of the plant water potential and weight of shoot and reserves for this first is found to be small. The crop weight has a coefficient of variation $CV \approx 0.02$ compared to a coefficient of variation of matric potential $CV \approx 0.15$ and of concentration $CV \approx 0.10$, resulting from a $CV \approx 1.3$ of the saturated hydraulic conductivity.

In a second example, a uniform concentration profile at 3000 mg l^{-1} is used. Irrigation is applied at a rate of 6 cm day^{-1} for 7 h every 7 days (1.75 cm water applied 10 times during the growing season). The results, using the linearization method are shown in Fig. 4. The ψ profiles again show less variance at wet soil conditions. The profiles on days 200, 225, and 250 are three days after, during, and four days after irrigation, respectively. The concentration profiles show gradual leaching of the salts and small concentration variances.

In the previous examples K_s was modeled as a uniform over depth but random variable and perfect correlation was imposed among different nodes. A different correlation function was also used, describing a randomly layered soil in the form $\mathbf{P}_{K_s}(\chi) = \sigma^2_{K_s} \times \exp\{-|\chi|/\chi_c\}$, where χ is the distance between nodes and χ_c is the correlation scale. The result is similar to the perfect correlation case (Fig. 3) but smaller variances are predicted.

For the results in Fig. 3 the coefficient of variation of K_s is around 1.3. Similar output uncertainty results for much smaller coefficients of variation for the cap-

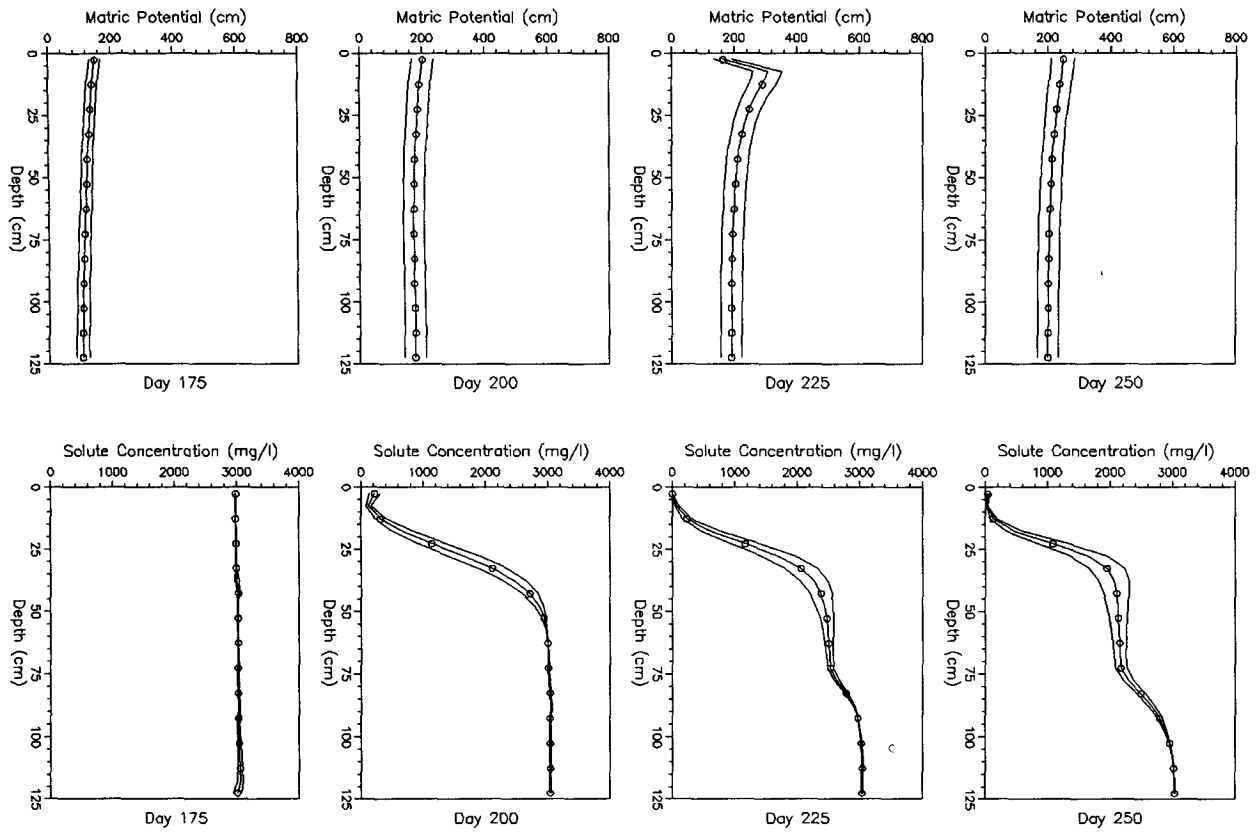

FIG. 4. Mean ± one-standard-deviation profiles of matric potential (upper part) and solute concentration (lower part), using the linearization method (K_s perfectly correlated over depth) ($c_0 = 3000$ mg l^{-1}, $r = 6$ cm day^{-1}).

illarity indices of conductivity α ($CV \approx 0.25$) and of moisture β ($CV \approx 0.30$), suggesting the importance of the variability of these parameters. The effect of the soil parameters is found to be almost additive to output variance: using these CVs for the parameters, assumed uncorrelated with each other, doubles the CVs of the output variables.

7. Summary and conclusions

In this paper a methodology is proposed for computing the variance of soil- and plant-state variables due to deviations of climatic variables and of soil parameters from their mean values. A linear model for the perturbations of the state and the inputs around the nominal (first-order mean) values is derived. The linear model is then used for uncertainty propagation. Based on statistical studies of daily weather data and weather simulation models we find that the random sequences of climatic variables can be represented during each day as products of a random amplitude and a deterministic shaping function. Such sequences are correlated at different time steps during a day with separable covariance function. The linearized model of the system is then used to propagate uncertainty. In a case study the relative importance of each climatic variable is quantified. It is found that correlation of climatic inputs from day to day increases the crop yield variance. The uncertainty of the climatic inputs does not affect significantly the soil-state variables. The results indicate that it is possible to predict risk in agricultural activities for different nominal climates. The model can be used to obtain the crop response and the associated risk for different initial conditions and irrigation practices.

The linearized model accepts different parameterizations of soil hydraulic parameters. The state perturbations are given as the product of a total sensitivity matrix and of the soil parameter perturbations. The correlation scale of the output variables is also computed. It is found that uncertainty reduces significantly as the soil parameters are used to obtain the soil-state variables and then the plant-state variables. These results are compared against results obtained using a Monte Carlo method and a qualitative agreement is found.

The results of this study indicate that only correlated sequences of climatic variables create significant effects

on biomass production and that the uncertainty of soil parameters is attenuated through the system dynamics. Both findings may suggest that natural vegetation systems have the capacity to resist moderate climatic changes and maintain their stability.

Acknowledgments. This research was initiated at Parsons Laboratory for Water Resources and Hydrodynamics, Department of Civil Engineering, Massachusetts Institute of Technology, and was sponsored by the National Science Foundation Grant CEE8211469 and the Massachusetts Institute of Technology Technological Planning Program, which was funded through a grant from the Agency for International Development, U.S. Department of State.

APPENDIX A

Effect of Correlation Structure on Output Variance—A Scalar Example

Consider the scalar system $x(\kappa + 1) = x(\kappa) + \xi(\kappa)$ with $E[x(0)] = 0$, $\text{var}[x(0)] = 0$, and $\xi(\kappa)$ a random process. Equivalently $x(\kappa + 1)$ can be written as the sum of $\kappa + 1$ random variables $\xi(0), \xi(1), \ldots, \xi(\kappa)$, or

$$x(\kappa + 1) = \sum_{i=0}^{\kappa} \xi(i).$$

Case 1. White noise input process

Let $\xi(\kappa) = \epsilon(\kappa)$ with $\epsilon(\kappa)$ zero mean, white noise with variance $r^2 = 1.0$. Since $\xi(i)$ are uncorrelated, identically distributed random variables, it follows that

$$\text{var}[x(\kappa)] = \sum_{i=0}^{\kappa-1} \text{var}[\xi(i)] = \sum_{i=0}^{\kappa-1} r^2 = \kappa r^2 = \kappa.$$

Thus the output variance increases linearly with time.

Let the input process be generated from $\xi(\kappa) = f(\kappa)n(\kappa)$, where $f(\kappa) = |\sin(\kappa/D)|$ is a deterministic shaping function within each cycle of length $D = 10.0$, and $n(\kappa)$ is a random amplitude sampled every D steps from the noise $\epsilon(\kappa)$ so that $n(\kappa) = n(\mu D) = \epsilon(\mu D)$ (no correlation among cycles), or generated from noise $\epsilon(\kappa)$ according to $n(\kappa) = n(\mu D) = \phi n[(\mu - 1)D] + (1 - \phi^2)^{1/2}\epsilon(\mu D)$ (lag-one correlation coefficient among cycles is ϕ).

Case 2. No correlation among cycles

Here,

$$\text{cov}[\xi(\kappa), \xi(s)] = \begin{cases} f(\kappa)f(s) & \text{for } \kappa, s \text{ in } [\mu D, (\mu + 1)D - 1] \\ 0 & \text{otherwise.} \end{cases}$$

The recursive procedure becomes

$$\text{var}[x(\kappa + 1)] = \text{var}[x(\kappa)] + f^2(\kappa) + 2N(\kappa)f(\kappa),$$
$$N(\kappa) = N(\kappa - 1) + \text{var}^{1/2}[\xi(\kappa - 1)]$$
$$= N(\kappa - 1) + f(\kappa - 1),$$
$$N(\mu D) = 0 \text{ and } \kappa \text{ in } [\mu D, (\mu + 1)D - 1].$$

Alternatively, the output variance can be computed directly, using the expression for a sum of correlated random variables (Benjamin and Cornell 1970) as

$$\text{var}[x(\kappa + 1)] = \sum_{i=0}^{\kappa} f^2(i) + 2 \sum_{j=\mu D}^{\kappa} \sum_{i=\mu D}^{i-1} f(i)f(j).$$

Case 3. Correlation among cycles

The recursive procedure is as in case 2, but $N(0) = 0$, and $N(\mu D) = \phi N(\mu D)$. The direct procedure for the variance of the sum of correlated random variables gives

$$\text{var}[x(\kappa + 1)] = \sum_{i=0}^{\kappa} f^2(i) + 2 \sum_{j=0}^{\kappa} \sum_{i=0}^{i-1} \phi^{\|i/D\| - \|j/D\|} f(i)f(j),$$

where $\|\cdot\|$ denotes integer part.

Sample paths of the processes defined in cases 1, 2, and 3 are shown in Fig. A.1. The output variance as a function of time is also shown. It is verified that the results of the recursive (solid line) and the direct method (square symbols) are identical. For the simple integrator system used in this example the output variance increases as the input has more and more memory.

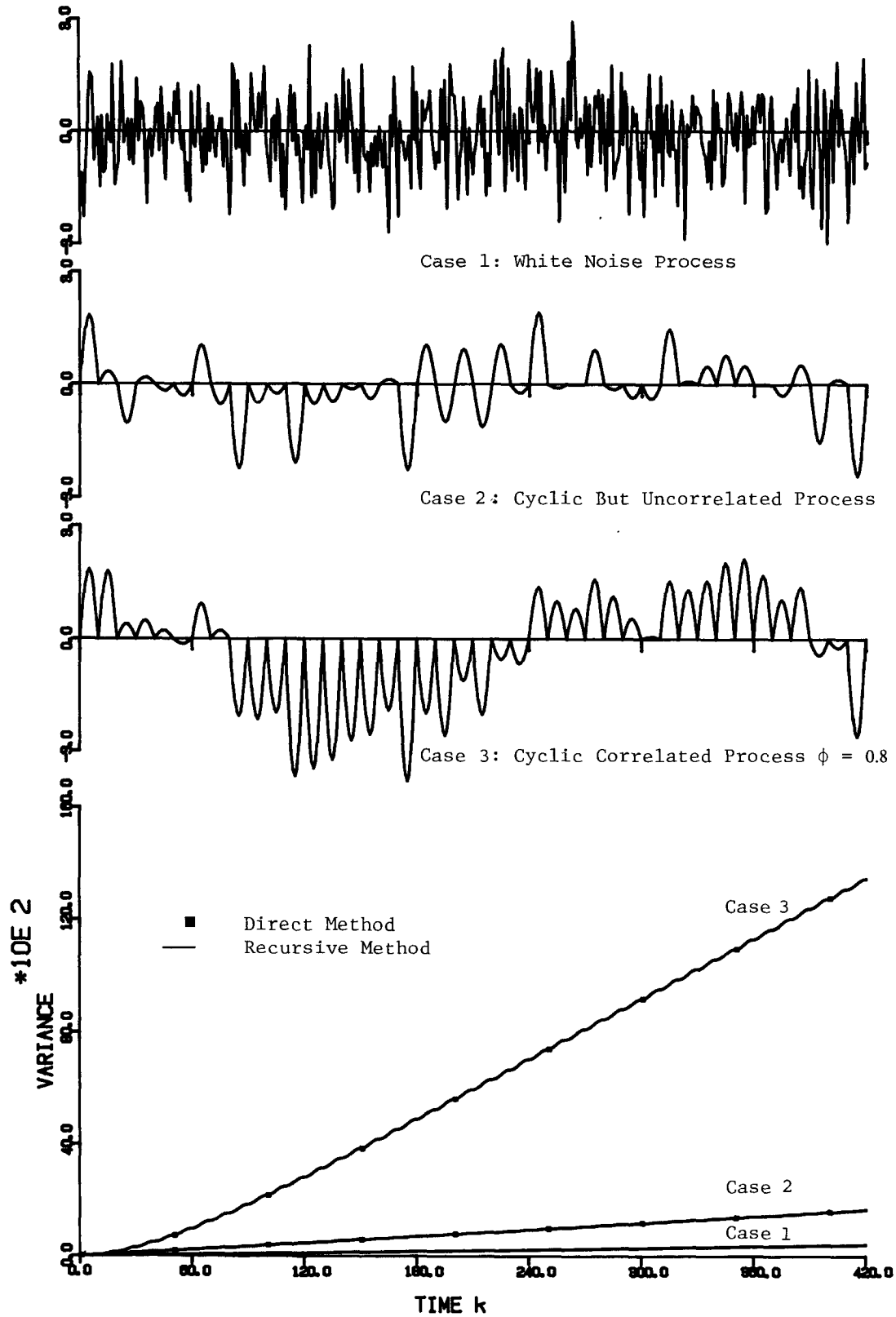

FIG. A.1. Sample paths of input process and output variance for scalar integrator example.

REFERENCES

Benjamin, J. R., and C. A. Cornell, 1970: *Probability, Statistics, and Decision for Civil Engineers.* McGraw Hill.

Bras, R. L., and I. Rodriguez-Iturbe, 1985: *Random Functions and Hydrology.* Addison-Wesley.

Bresler, E., and G. Dagan, 1988a: Variability of yield of an irrigated crop and its causes. Part I: Statement of the problem and Methodology. *Water Resour. Res.*, **24,** 381–387.

——, and ——, 1988b: Variability of yield of an irrigated crop and its causes. Part II: Input data and illustration of results. *Water Resour. Res.*, **24,** 389–394.

——, S. Dasberg, D. Russo, and G. Dagan, 1981: Spatial variability of crop yield as a stochastic soil process. *Soil Sci. Soc. Am. J.*, **45,** 600–605.

Childs, S. W., J. R. Gilley, and W. E. Splinter, 1977: A simplified model of corn growth under moisture stress. *Trans. A.S.A.E.*, 858–865.

Dagan, G., and E. Bresler, 1988: Variability of yield of an irrigated crop and its causes. Part III: Numerical simulation and field results. *Water Resour. Res.*, **24,** 394–401.

de Wit, C. T., et al., 1978: *Simulation of Assimilation, Respiration and Transpiration of Crops.* Wiley.

Eagleson, P. S., 1978a: Climate, Soil and Vegetation. Part I: Introduction to water balance dynamics. *Water Resour. Res.*, **14,** 705–712.

——, 1978b: Climate, Soil and Vegetation. Part II: The distribution of annual precipitation derived from observed storm sequences. *Water Resour. Res.*, **14,** 712–721.

——, 1978c: Climate, Soil and Vegetation. Part III: A simplified model of soil moisture movement in the liquid phase. *Water Resour. Res.*, **14,** 722–730.

——, 1978d: Climate, Soil and Vegetation. Part IV: The expected value of annual evapotranspiration. *Water Resour. Res.*, **14,** 731–740.

——, 1978e: Climate, Soil and Vegetation. Part V: A derived distribution of storm surface runoff. *Water Resour. Res.*, **14,** 741–748.

——, 1978f: Climate, Soil and Vegetation. Part VI: Dynamics of the annual water balance. *Water Resour. Res.*, **14,** 749–764.

——, 1978g: Climate, Soil and Vegetation. Part VII: A derived distribution of annual water yield. *Water Resour. Res.*, **14,** 765–775.

Gustavson, F. G., 1978: Two fast algorithms for sparse matrices: Multiplication and permuted transposition. *ACM Trans. Math. Software,* **4,** 250–268.

Huck, M. G., and D. Hillel, 1983: A model of root growth and water uptake accounting for photosynthesis, respiration, transpiration and soil hydraulics. *Adv. Irrig.*, **2,** 273–333.

Protopapas, A. L., 1988: Stochastic hydrologic analysis of soil–crop–climate interactions. Ph.D. thesis, Dept. of Civil Engineering, Massachusetts Institute of Technology, Cambridge, Mass.

——, and R. L. Bras, 1987: A model for water uptake and development of root systems. *Soil Sci.*, **144,** 352–366.

——, and ——, 1988: State-space dynamic hydrological modeling of soil–crop–climate interactions. *Water Resour. Res.*, **24,** 1765–1779.

——, and ——, 1990: Uncertainty propagation with numerical models for flow and transport in the unsaturated zone. *Water Resour. Res.*, **26,** 2463–2474.

Ritchie, J. T., and S. Otter, 1985: Description and performance of CERES-Wheat: A user-oriented wheat yield model. *ARS Wheat Yield Project,* U.S. Department of Agriculture, ARS-38.

Russo, D., 1983: A geostatistical approach to the trickle irrigation design in heterogeneous soil. Part I: Theory. *Water Resour. Res.*, **19,** 632–642.

——, 1984a: A geostatistical approach to the trickle irrigation design in heterogeneous soil. Part II: A field test. *Water Resour. Res.*, **20,** 543–552.

——, 1984b: Statistical analysis of crop yield—soil water relationships in heterogeneous soil under trickle irrigation. *Soil Science Soc. Amer. J.*, **46,** 1402–1410.

——, 1986: A stochastic approach to the crop yield—irrigation relationships in heterogeneous soils. Part I: Analysis of the field spatial variability. *Soil Science Soc. Amer. J.*, **50,** 736–745.

——, 1988: Determining soil hydrolic properties by parameter estimation: On the selection of a model for the hydrolic properties. *Water Resour. Res.*, **24,** 453–459.

Warrick, A. W., and W. R. Gardner, 1983: Crop yield as affected by spatial variations of soil and irrigation. *Water Resour. Res.*, **19,** 181–186.

——, J. W. Biggar, and D. R. Nielsen, 1971: Simultaneous solute and water transfer for an unsaturated soil. *Water Resour. Res.*, **7,** 1216–1225.

Whittle, P., 1956: On the variation of yield variance with plot size. *Biometrika,* **43,** 337–343.

Zur, B., and J. W. Jones, 1981: A model for the water relations, photosynthesis, and expansive growth of crops. *Water Resour. Res.*, **17,** 311–320.